International Journal of Materials Engineering and Technology

http://www.pphmj.com
http://dx.doi.org/10.17654/0975044423005
Volume 22, Number 1, 2023, Pages 55-83 **P-ISSN: 0975-0444**

THEORETICAL AND NUMERICAL ANALYSES OF SHORT NATURAL FIBERS ORIENTATION IN THERMOPLASTIC MATRIX

I. Modhaffar[1], K. Gueraoui[1,2], M. Taibi[1,3], H. El-Tourroug[1] and S. Men-La-Yakhaf[1]

[1]Team of Modelling and Simulating of Mechanical and Energetic (MSME)
Faculty of Science
Mohammed V University
Rabat, Morocco

[2]Department of Mechanical Engineering
University of Ottawa
Ottawa, K1N 6N5, Canada

[3]Laboratory of Mechanics
Faculty Ain Chock of Science
Hassan II University
Casablanca, Morocco

Received: February 1, 2023; Revised: February 22, 2023; Accepted: March 23, 2023

Keywords and phrases: short fiber, orientation, polymer, numerical simulation, Runge-Kutta method thermoplastic, Folgar, Tucker, Jeffery.

How to cite this article: I. Modhaffar, K. Gueraoui, M. Taibi, H. El-Tourroug and S. Men-La-Yakhaf, Theoretical and numerical analyses of short natural fibers orientation in thermoplastic matrix, International Journal of Materials Engineering and Technology 22(1) (2023), 55-83. http://dx.doi.org/10.17654/0975044423005

Published Online: June 17, 2023

Abstract

In this article, we presented a complete mathematical model based on Jeffery, Folgar-Tucker model and kinematics of fiber-orientation. Such a model helps to determine the orientation of the short fibers in the molding process, as well as the different physical parameters which influence the studied phenomenon. We are interested in the analysis of the orientation of short fibers in a thermoplastic matrix, through numerical simulation during injection molding of the composite polymer. The orientation of the fibers is usually determined by the coupling flow (fibers-thermoplastic matrix), the flow temperature, and the free movement region of the equation's kinematic fibers for flow direction. The second-order orientation tensor defines the cinematic of a group of fibers. This analysis is supported by experiential findings.

0. Introduction

The manufacture of a polymer (polypropylene) is extruded and then cooled in a desired form, reinforced with short fiber. During this fabrication process, the orientation of the fibers changes and the final pattern is maintained in the part after the solidification phase of the matrix.

The two-dimensional research on a given group of fibers makes it possible to understand the history of the orientation of the latter one during mold filling. We are especially interested in the fibers that are subjected to the flow of the fountain before the material. Thermal conditions and shear thinning behavior affect the fiber paths, and hence the final orientations of the fibers.

Considering the interaction of the fibers results in a slight disorientation from the part's plane, making the shear flows effective in orienting the fibers towards the flow direction. The precise kinematic calculation allows testing for the orientation of the fibers and the constitutive equations of other physical models. Tracking of individual fibers should be replaced by a continuous orientation description to obtain an image across the filled domain that can be compared to experiments conducted in the transverse

direction of flow and flow thickness, respectively. Recently, various studies have been done to obtain relationships between fiber orientation and processing state. Jeffery [1] was the first to work on fiber suspension flow and discover the distribution function of the orientation angle of the particle. Jeffery assumes, in his model, that the particle is rigid, neutral, progressive, and broad enough for the motion to be Brownian.

Lipscomb [2] and Bay [7] suggested a constitutive equation with a high aspect ratio for dilute suspensions of ellipsoidal particles.

The Folgar and Tucker model [8] takes into account Jeffery's implemented fiber-fiber interaction coefficient.

The originality of this work lies in that it enables the average orientation of short fibers to be calculated in polypropylene, strengthened by natural fibers. The movement of the fiber-fluid assembly has been studied by the classical fluid mechanics equations (conservation of mass, momentum, and energy) coupled with the Jeffery, Folgar, and Tucker model equations. By using the second-order Runge-Kutta method coupled with finite difference method, the above equations are solved. Using a program on Matlab, we determined the various orientations of the short fibers using image processing.

1. Mathematical Formulation

1.1. Study hypotheses

The following hypotheses are considered in relation to this study:

- The pipe wall is considered to be rigid and impermeable, and the gravity effect is neglected.
- The composite material is a dilute or semi-concentrated suspension in the molten state.
- The matrix of polymers is Newtonian.
- The fiber dimensions are negligible when compared with the flow dimensions.

• Brownian diffusion due to the interaction of fibers is neglected.

1.2. Equation of fluid motion

The motion of a fluid such as a polymer can be defined by a series of partial differential equations derived from the fundamental laws of mechanics and thermodynamics, i.e., the laws of mass conservation (equation continuity), momentum (momentum equations), and energy (energy equation).

- Conservation of mass:

$$\frac{\partial \rho}{\partial t} + \nabla(\rho \cdot \vec{v}) = 0. \tag{1}$$

- Conservation the amount of movement:

$$\frac{\partial(\rho\vec{v})}{\partial t} + \vec{\nabla} \cdot (\rho\vec{v} \cdot \vec{v}) = -\overline{\nabla}_p + \vec{\nabla} \cdot \bar{\bar{\tau}} + \rho\vec{f}. \tag{2}$$

- Energy conservation:

$$\frac{\partial e}{\partial t} + \vec{v}(\vec{\nabla} e) + \frac{1}{\rho}\vec{v}(\vec{\nabla} P) = \frac{\mu}{\rho}(\nabla^2\vec{v}) \cdot \vec{v} + \frac{\lambda}{\rho}(\nabla^2 T). \tag{3}$$

Taking into account the hypothesis of incompressibility of the polymer and projection on the Cartesian axes, these equations become

$$\frac{\partial V_x}{\partial x} + \frac{\partial V_y}{\partial y} = 0 \tag{4}$$

and

$$\begin{cases} \dfrac{\partial V_x}{\partial t} + V_x \dfrac{\partial V_x}{\partial x} + V_y \dfrac{\partial V_x}{\partial y} = -\dfrac{1}{\rho}\dfrac{\partial P}{\partial x} + \upsilon\left(\dfrac{\partial^2 V_x}{\partial x^2} + \dfrac{\partial^2 V_x}{\partial y^2}\right), & (5) \\ \dfrac{\partial V_y}{\partial t} + V_x \dfrac{\partial V_y}{\partial x} + V_y \dfrac{\partial V_y}{\partial y} = -\dfrac{1}{\rho}\dfrac{\partial P}{\partial y} + \upsilon\left(\dfrac{\partial^2 V_y}{\partial x^2} + \dfrac{\partial^2 V_y}{\partial y^2}\right). & (6) \end{cases}$$

Since of symmetry and the source term is negligible, the energy equation is written as:

$$\rho\frac{\partial e}{\partial t}+V_x\left(\frac{\partial e}{\partial x}+\frac{1}{\rho}\frac{\partial P}{\partial x}\right)+V_y\left(\frac{\partial e}{\partial y}+\frac{1}{\rho}\frac{\partial P}{\partial y}\right)$$

$$=\upsilon\left(V_x\frac{\partial^2 V_x}{\partial x^2}+V_x\frac{\partial^2 V_y}{\partial y^2}\right)+\frac{\lambda}{\rho}\left(\frac{\partial^2 T}{\partial x^2}+\frac{\partial^2 T}{\partial y^2}\right). \quad (7)$$

For our case, the fluid is incompressible. Therefore the internal energy is connected to the temperature by the relation:

$$de = c_v dT,$$

where c_v is the specific heat at constant volume.

Equation (7) becomes

$$C_v\frac{\partial T}{\partial t}+C_v\left(V_x\frac{\partial T}{\partial x}+V_y\frac{\partial T}{\partial y}\right)+\left(\frac{V_x}{\rho}\frac{\partial P}{\partial x}+\frac{V_y}{\rho}\frac{\partial P}{\partial y}\right)$$

$$=\upsilon\left(V_x\frac{\partial^2 V_x}{\partial x^2}+V_y\frac{\partial^2 V_y}{\partial y^2}\right)+\frac{\lambda}{\rho}\left(\frac{\partial^2 T}{\partial x^2}+\frac{\partial^2 T}{\partial y^2}\right). \quad (8)$$

The fluid is modeled by the following Arrhenius law:

$$\eta=\eta_0(T_{réf})e^{A_{réf}\left(\frac{1}{T}-\frac{1}{T_{réf}}\right)},$$

where $A_{réf}$ represents the ratio of activation energy, λ the assumed constant thermal conductivity, η_0 the reference viscosity and $T_{réf}$ the reference temperature.

1.3. Boundary conditions

In view of equations (5), (6) and (8), we add the following boundary conditions:

$$\left.\frac{\partial V_y}{\partial x}\right|_{x=0}=0,$$

$$V_y\big|_{x=1}=0,$$

$$\left.\frac{\partial T}{\partial x}\right|_{x=0} = 0,$$

$$T(x = l) = T_P,$$

where T_P is the temperature at the wall of the pipe.

2. Modeling the Orientation of Flowing Fibers

2.1. Description of orientation

Each fiber can be represented by a unit vector $\vec{P}$ ported by its main axis.

We can thus define the orientation of a fiber by the projection of the vector $\vec{P}$ in a fixed frame. The components of this vector are related to the angles θ and ϕ by:

$$\begin{cases} P_1 = \sin\theta\cos\phi, \\ P_2 = \sin\theta\sin\phi, \\ P_3 = \cos\theta. \end{cases} \quad (9)$$

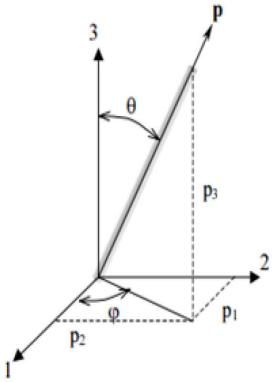

Figure 1. Angles and the vector characterizing the orientation of a fiber.

Figure 1 defines the angles and the vector characterizing the orientation of a fiber. In the literature, these angles are defined in a conventional way [7-9] such as:

- the angle θ, called the *angle of inclination*, is the angle formed from the z axis to the direction of the fiber;

- the angle φ or an *azimuthal angle* is defined in the *XY* plane with respect to the *x* axis.

The fiber reinforcement in the case of short-fiber composites usually consists of a very large number of fibers. Therefore, by means of an orientation probability density function, it is useful to define the overall orientation of a suspension, then the distribution function provides a general and precise definition of the orientation condition of a suspension at a given material point.

2.2. Evolution model of a single fiber

Jeffery [1] measured a single ellipsoidal particle immersed in a Newtonian fluid flow. The key assumption is that the particle dimensions are small enough that the area of strain rate is homogeneous over a large distance, and that the inertia forces are ignored.

Reference [10] updated Jeffery's equation to take account of the interactions between fibers. The evolution of a single fiber's orientation is then:

$$\frac{\overrightarrow{\partial p}}{\partial t} + v\nabla\vec{P} = \Omega(v)\vec{P} + \lambda(\varepsilon(v)\vec{P} - (\varepsilon(v) : \vec{P} \otimes \vec{P})\vec{P}) - \frac{D_r}{\psi}\frac{\partial\Psi}{\partial\vec{P}}, \qquad (10)$$

where $(:)$ denotes the contracted product doubly.

ψ represents the orientation distribution function defined above and D_r is the Brownian coefficient of diffusion, v is the local velocity field, Ω and ε are, respectively, the tensors of rotation and strain rates defined by

$$\Omega(v) = \frac{1}{2}\left(\frac{\partial v_i}{\partial X_j} - \frac{\partial v_j}{\partial X_i}\right), \quad \varepsilon(v)_{i,j} = \frac{1}{2}\left(\frac{\partial v_i}{\partial X_j} + \frac{\partial v_j}{\partial X_i}\right).$$

The parameter λ is a function of the aspect ratio of the fibers β (ratio between the average length L and the average diameter D of the fibers) and is given by

$$\lambda = \frac{\beta^2 - 1}{\beta^2 + 1}; \quad \beta = \frac{L}{D}.$$

Brownian diffusion due to the interaction of fibers is neglected. Equation (10) becomes

$$\frac{\overrightarrow{\partial p}}{\partial t} + v\nabla\vec{P} = \Omega(v)\vec{P} + \lambda(\varepsilon(v)\vec{P} - (\varepsilon(v) : \vec{P} \otimes \vec{P})\vec{P}).$$

Note that

$$\vec{P} = \begin{cases} P_x \\ P_y \\ 0. \end{cases}$$

Projecting along the x and y axes, the equations take the following form:

$$\frac{\partial P_x}{\partial t} + v_x \frac{\partial P_x}{\partial x} = -\frac{1}{2} P_y \left(\frac{\partial v_y}{\partial x} - \frac{\partial v_x}{\partial y} \right) + \lambda P_x \frac{\partial v_x}{\partial x} (1 - P_x^2 - P_y^2)$$

$$+ \frac{1}{2} P_y \lambda \left(\frac{\partial v_x}{\partial y} + \frac{\partial v_y}{\partial x} \right) (1 - P_x^2 - P_y^2), \tag{11}$$

$$\frac{\partial P_y}{\partial t} + v_y \frac{\partial P_y}{\partial y} = \frac{1}{2} P_x \left(\frac{\partial v_y}{\partial x} - \frac{\partial v_x}{\partial y} \right) + \lambda P_y \frac{\partial v_y}{\partial y} (1 - P_x^2 - P_y^2)$$

$$+ \frac{1}{2} P_x \lambda \left(\frac{\partial v_x}{\partial y} + \frac{\partial v_y}{\partial x} \right) (1 - P_x^2 - P_y^2). \tag{12}$$

2.3. Evolution models of a fiber population

Several authors [11-13] measured the movement of fiber in reinforced thermoplastics directly for the orientation measurement of a population of fibers. This is why it was more valid to use a compact notation of fiber orientation (orientation tensors) and to build macroscopic models that allowed the evolution of these tensors to be followed.

Reference [14] used the equation of Jeffery to model the orientation state of a fiber population. This equation was homogenized in volume and combined with the Fokker-Plank equation to give a second-order orientation tensor evolution equation:

$$\frac{\partial a}{\partial t} + v\nabla a = \Omega(v)a - a\Omega(v) + \lambda(\varepsilon(v)\cdot a + (a\cdot\varepsilon(v) - 2\varepsilon(v) : A)). \quad (13)$$

Equation (13) is only valid for dilute suspensions (interactions between fibers are neglected).

Projecting along the x and y axes, the equations take the following form:

•

$$\frac{\partial a_{11}}{\partial t} + V_k \frac{\partial a_{11}}{\partial x_k} = -(\varepsilon_{1k}a_{k1} - a_{1k}\varepsilon_{k1}) + \lambda(\Omega_{1k}a_{k1} + a_{1k}\Omega - 2\Omega_{kl}A_{11kl}).$$

•

$$\frac{\partial a_{12}}{\partial t} + V_x \frac{\partial a_{12}}{\partial x_k} = -(\varepsilon_{1k}a_{k2} - a_{1k}\varepsilon_{k2}) + \lambda(\Omega_{1k}a_{k2} + a_{1k}\Omega_{k2} - 2\Omega_{kl}A_{12kl}).$$

•

$$\frac{\partial a_{22}}{\partial t} + V_x \frac{\partial a_{22}}{\partial x_k} = -(\varepsilon_{2k}a_{k2} - a_{2k}\varepsilon_{k2}) + \lambda(\Omega_{2k}a_{k2} + a_{2k}\Omega_{k2} - 2\Omega_{kl}A_{22kl}).$$

These equations become

• $$\frac{\partial a_{11}}{\partial t} + V_x \frac{\partial a_{11}}{\partial x} + V_y \frac{\partial a_{11}}{\partial y} = -2\lambda\Omega_{kl}A_{11kl}, \quad (14)$$

•

$$\begin{aligned}
&\frac{\partial a_{12}}{\partial t} + V_x \frac{\partial a_{12}}{\partial x} + V_y \frac{\partial a_{12}}{\partial y} \\
&= \left[\frac{1}{2}\frac{\partial v_y}{\partial x}(1+\lambda) + \frac{1}{2}\frac{\partial v_x}{\partial y}(1-\lambda)\right]a_{11} + \left(\frac{\partial v_y}{\partial y} - \frac{\partial v_x}{\partial x}\right)a_{12} \\
&\quad + \left[\frac{1}{2}\frac{\partial v_y}{\partial x}(\lambda-1) - \frac{1}{2}\frac{\partial v_x}{\partial y}(\lambda+1)\right]a_{22} - 2\lambda\Omega_{kl}A_{12kl}, \quad (15)
\end{aligned}$$

• $$\frac{\partial a_{22}}{\partial t} + V_x \frac{\partial a_{22}}{\partial x} + V_y \frac{\partial a_{22}}{\partial y} = -2\lambda\Omega_{kl}A_{22kl}. \quad (16)$$

3. Resolution Method

The basic equations that govern the issue are not linear, and are coupled. They do not usually accept empirical solutions, except in extremely simplified situations. The use of numerical methods is therefore important. We have chosen to use the implicit second-order Runge-Kutta method coupled with the finite differential method in the present simulation.

These procedures include two phases: mesh and discretization.

3.1. Mesh

In two dimensions, the domain is subdivided into a finite number of control volumes which are made up of regular surface elements.

A mesh has the following form:

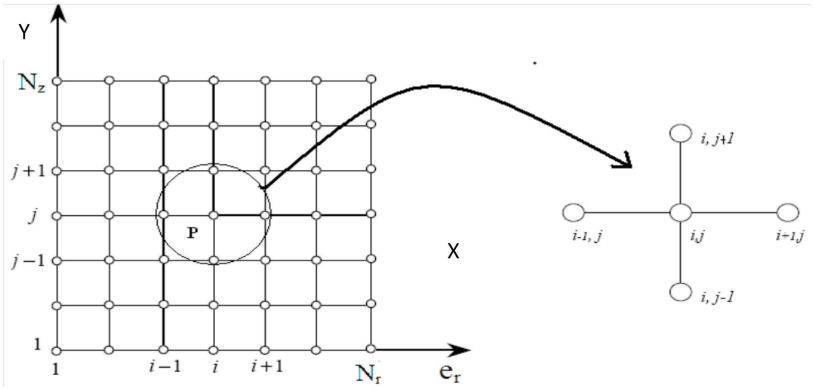

Figure 2

where P is the main node, i is the discretization index along the "x" axis, and j is the discretization index along the "z" axis.

Subsequently, we adopt the following meshes:

$$x(i) = (i-1)\Delta x,$$

$$z(i) = (j-1)\Delta z.$$

3.2. Discretizations

3.2.1. Momentum balance equation

Equation (5) becomes

$$\frac{\partial V_x}{\partial t} = f(V_x)$$

with

$$f(V_x) = -V_x \frac{\partial V_x}{\partial x} - V_y \frac{\partial V_x}{\partial y} - \frac{1}{\rho}\frac{\partial P}{\partial x} + \upsilon\left(\frac{\partial^2 V_x}{\partial x^2} + \frac{\partial^2 V_x}{\partial y^2}\right).$$

According to the second-order Runge-Kutta method, this equation is written as:

$$V_x^{k+1}(i,\ j) = V_x^k(i,\ j) + \Delta t f(V_x^{k+1/2}(i,\ j))$$

or

$$V_x^{k+1/2}(i,\ j) = V_x^k(i,\ j) + \frac{\Delta t}{2} f(V_x^k(i,\ j))$$

with

$$f(V_x^k(i,\ j)) = -V_x^k(i,\ j)\frac{V_x^k(i+1,\ j) - V_x^k(i-1,\ j)}{2\Delta x}$$

$$- V_y^k(i,\ j)\frac{V_x^k(i,\ j+1) - V_x^k(i,\ j-1)}{2\Delta y} - \frac{1}{\rho}\frac{\partial P}{\partial x}\Bigg)_{(i,\ j)}^{k}$$

$$+ \upsilon\left(\frac{V_x^k(i+1,\ j) - 2V_x^k(i,\ j) + V_x^k(i-1,\ j)}{\Delta x^2}\right.$$

$$\left. + \frac{V_x^k(i,\ j+1) - 2V_x^k(i,\ j) + V_x^k(i,\ j-1)}{\Delta y^2}\right)$$

and

$$f(V_x^{k+1/2}(i,\ j)) = -V_x^{k+1/2}(i,\ j)\frac{V_x^{k+1/2}(i+1,\ j)-V_x^{k+1/2}(i-1,\ j)}{2\Delta x}$$
$$- V_y^{k}(i,\ j)\frac{V_x^{k+1/2}(i,\ j+1)-V_x^{k+1/2}(i,\ j-1)}{2\Delta y} - \frac{1}{\rho}\frac{\partial P}{\partial x}\Bigg)_{(i,\ j)}^{k}$$
$$+ \upsilon\Bigg(\frac{V_x^{k+1/2}(i+1,\ j) - 2V_x^{k+1/2}(i,\ j) + V_x^{k+1/2}(i-1,\ j)}{\Delta x^2}$$
$$+ \frac{V_x^{k+1/2}(i,\ j+1) - 2V_x^{k+1/2}(i,\ j) + V_x^{k+1/2}(i,\ j-1)}{\Delta y^2}\Bigg).$$

Similarly equation (6) becomes

$$\frac{\partial V_y}{\partial t} = f(V_y)$$

with

$$f(V_y) = -V_x\frac{\partial V_y}{\partial x} - V_y\frac{\partial V_y}{\partial y} - \frac{1}{\rho}\frac{\partial P}{\partial y} + \upsilon\left(\frac{\partial^2 V_y}{\partial x^2} + \frac{\partial^2 V_y}{\partial y^2}\right).$$

According to the second-order Runge-Kutta method, this equation is written as:

$$V_y^{k+1}(i,\ j) = V_y^{k}(i,\ j) + \Delta t f(V_y^{k+1/2}(i,\ j))$$

or

$$V_y^{k+1/2}(i,\ j) = V_y^{k}(i,\ j) + \frac{\Delta t}{2} f(V_y^{k}(i,\ j))$$

with

$$f(V_y^{k}(i,\ j)) = -V_x^{k}(i,\ j)\frac{V_y^{k}(i+1,\ j) - V_y^{k}(i-1,\ j)}{2\Delta x}$$
$$- V_y^{k}(i,\ j)\frac{V_y^{k}(i,\ j+1) - V_y^{k}(i,\ j-1)}{2\Delta y} - \frac{1}{\rho}\frac{\partial P}{\partial y}\Bigg)_{(i,\ j)}^{k}$$

$$+\upsilon\left(\frac{V_y^k(i+1,\ j)-2V_y^k(i,\ j)+V_y^k(i-1,\ j)}{\Delta x^2}\right.$$

$$\left.+\frac{V_y^k(i,\ j+1)-2V_y^k(i,\ j)+V_y^k(i,\ j-1)}{\Delta y^2}\right)$$

and

$$f(V_x^{k+1/2}(i,\ j))=-V_x^{k+1/2}(i,\ j)\frac{V_y^{k+1/2}(i+1,\ j)-V_y^{k+1/2}(i-1,\ j)}{2\Delta x}$$

$$-V_y^k(i,\ j)\frac{V_y^{k+1/2}(i,\ j+1)-V_y^{k+1/2}(i,\ j-1)}{2\Delta y}-\frac{1}{\rho}\frac{\partial P}{\partial y}\Bigg)_{(i,\ j)}^{k}$$

$$+\upsilon\left(\frac{V_y^{k+1/2}(i+1,\ j)-2V_y^{k+1/2}(i,\ j)+V_y^{k+1/2}(i-1,\ j)}{\Delta x^2}\right.$$

$$\left.+\frac{V_y^{k+1/2}(i,\ j+1)-2V_y^{k+1/2}(i,\ j)+V_y^{k+1/2}(i,\ j-1)}{\Delta y^2}\right).$$

3.2.2. Energy balance equation

Equation (8) becomes

$$\frac{\partial T}{\partial t}=f(t)$$

with

$$f(T)=-\left(V_x\frac{\partial T}{\partial x}+V_y\frac{\partial T}{\partial y}\right)-\frac{1}{\rho C_v}\left(V_x\frac{\partial P}{\partial x}+V_y\frac{\partial P}{\partial y}\right)$$

$$+\frac{\upsilon}{C_v}\left(V_x\frac{\partial^2 V_x}{\partial x^2}+V_y\frac{\partial^2 V_y}{\partial y^2}\right)+\frac{\lambda}{\rho C_v}\left(\frac{\partial^2 T}{\partial x^2}+\frac{\partial^2 T}{\partial y^2}\right).$$

According to the second-order Runge-Kutta method, this equation is written as:

$$T^{k+1}(i,\ j) = T^{k}(i,\ j) + \Delta t\, f(T^{k+1/2}(i,\ j))$$

or

$$T^{k+1/2}(i,\ j) = T^{k}(i,\ j) + \frac{\Delta t}{2} f(T(i,\ j))$$

with

$$\begin{aligned} & f(T^{k}(i,\ j)) \\ &= -V_x(i,\ j)\frac{T^{k}_{(i+1,\ j)} - T^{k}_{(i-1,\ j)}}{2\Delta x} - V_y(i,\ j)\frac{T^{k}_{(i,\ j+1)} - T^{k}_{(i,\ j-1)}}{2\Delta y} \\ &\quad + \frac{\lambda}{\rho C_v}\left(\frac{T^{k}_{(i+1,\ j)} - 2T^{k}_{(i,\ j)} + T^{k}_{(i-1,\ j)}}{\Delta x^2} + \frac{T^{k}_{(i,\ j+1)} - 2T^{k}_{(i,\ j)} + T^{k}_{(i,\ j-1)}}{\Delta y^2}\right) \\ &\quad - \frac{1}{\rho C_v}\left(\left(V_x\frac{\partial P}{\partial x} + V_y\frac{\partial P}{\partial y}\right) - \rho\upsilon\left(V_x\frac{\partial^2 V_x}{\partial x^2} + V_y\frac{\partial^2 V_y}{\partial y^2}\right)\right)(i,\ j) \end{aligned}$$

and

$$\begin{aligned} & f(T^{k+1/2}(i,\ j)) \\ &= -V_x(i,\ j)\frac{T^{k+1/2}_{(i+1,\ j)} - T^{k+1/2}_{(i-1,\ j)}}{2\Delta x} - V_y(i,\ j)\frac{T^{k+1/2}_{(i,\ j+1)} - T^{k+1/2}_{(i,\ j-1)}}{2\Delta y} \\ &\quad - \frac{\lambda}{\rho C_v}\left(\frac{T^{k+1/2}_{(i+1,\ j)} - 2T^{k+1/2}_{(i,\ j)} + T^{k+1/2}_{(i-1,\ j)}}{\Delta x^2} + \frac{T^{k+1/2}_{(i,\ j+1)} - 2T^{k+1/2}_{(i,\ j)} + T^{k+1/2}_{(i,\ j-1)}}{\Delta y^2}\right) \\ &\quad - \frac{1}{\rho C_v}\left(\left(V_x\frac{\partial P}{\partial x} + V_y\frac{\partial P}{\partial y}\right) - \rho\upsilon\left(V_x\frac{\partial^2 V_x}{\partial x^2} + V_y\frac{\partial^2 V_y}{\partial y^2}\right)\right)(i,\ j). \end{aligned}$$

3.2.3. Fiber domain

- **Description of orientation**

Equation (11) becomes

$$\frac{\partial P_x}{\partial t} = f(P_x)$$

with

$$f(P_x) = -v_x \frac{\partial P_x}{\partial x} - \frac{1}{2} P_y \left(\frac{\partial v_y}{\partial x} - \frac{\partial v_x}{\partial y} \right) + \lambda P_x \frac{\partial v_x}{\partial x} (1 - P_x^2 - P_y^2)$$

$$+ \frac{1}{2} P_y \lambda \left(\frac{\partial v_x}{\partial y} + \frac{\partial v_y}{\partial x} \right) (1 - P_x^2 - P_y^2).$$

According to the second-order Runge-Kutta method, this equation is written as

$$P_x^{k+1}(i,\ j) = P_x^k(i,\ j) + \Delta t f(P_x^{k+1/2}(i,\ j))$$

or

$$P_x^{k+1/2}(i,\ j) = P_x^k(i,\ j) + \frac{\Delta t}{2} f(P_x(i,\ j))$$

with

$$f(P_x^k(i,\ j)) = -V_x(i,\ j) \frac{P^k_{x(i+1,\ j)} - P^k_{x(i-1,\ j)}}{2\Delta x} - \frac{1}{2} P_y^k(i,\ j) \left(\frac{\partial v_y}{\partial x} - \frac{\partial v_x}{\partial y} \right)^k (i,\ j)$$

$$+ \lambda P_x^k(i,\ j) \frac{\partial v_x}{\partial x} \Big)^k_{(i,\ j)} (1 - P_x^k(i,\ j)^2 - P_y^k(i,\ j)^2)$$

$$+ \frac{\lambda}{2} P_y^k(i,\ j) \left(\frac{\partial v_x}{\partial y} + \frac{\partial v_y}{\partial x} \right)^k (i,\ j) (1 - P_x^k(i,\ j)^2 - P_y^k(i,\ j)^2)$$

and

$$f(P_x^{k+1/2}(i,\ j))$$

$$= -V_x(i,\ j)\frac{P_{x(i+1,\ j)}^{k+1/2} - P_{x(i-1,\ j)}^{k+1/2}}{2\Delta x} - \frac{1}{2}P_y^k(i,\ j)\left(\frac{\partial v_y}{\partial x} - \frac{\partial v_x}{\partial y}\right)^k(i,\ j)$$

$$+ \lambda P_x^{k+1/2}(i,\ j)\frac{\partial v_x}{\partial x}\Bigg)_{(i,\ j)}^k (1 - P_x^{k+1/2}(i,\ j)^2 - P_y^k(i,\ j)^2)$$

$$+ \frac{\lambda}{2}P_y^k(i,\ j)\left(\frac{\partial v_x}{\partial y} + \frac{\partial v_y}{\partial x}\right)^k(i,\ j)(1 - P_x^{k+1/2}(i,\ j)^2 - P_y^k(i,\ j)^2).$$

Equation (12) becomes

$$\frac{\partial P_y}{\partial t} = f(P_y)$$

with

$$f(P_y) = -v_y\frac{\partial P_y}{\partial y} + \frac{1}{2}P_x\left(\frac{\partial v_y}{\partial x} - \frac{\partial v_x}{\partial y}\right) + \lambda P_y\frac{\partial v_y}{\partial y}(1 - P_x^2 - P_y^2)$$

$$+ \frac{1}{2}P_x\lambda\left(\frac{\partial v_x}{\partial y} + \frac{\partial v_y}{\partial x}\right)(1 - P_x^2 - P_y^2).$$

According to the second-order Runge-Kutta method, this equation is written as:

$$P_y^{k+1}(i,\ j) = P_y^k(i,\ j) + \Delta t f(P_y^{k+1/2}(i,\ j))$$

or

$$P_y^{k+1/2}(i,\ j) = P_y^k(i,\ j) + \frac{\Delta t}{2}f(P_y(i,\ j))$$

with

$$
\begin{aligned}
& f(P_y^k(i,\ j)) \\
&= -V_y(i,\ j)\frac{P^k_{y(i,\ j+1)} - P^k_{y(i,\ j-1)}}{2\Delta y} + \frac{1}{2}P_y^k(i,\ j)\left(\frac{\partial v_y}{\partial x} - \frac{\partial v_x}{\partial y}\right)^k(i,\ j) \\
&\quad + \lambda P_y^k(i,\ j)\frac{\partial v_y}{\partial y}\Bigg)^k_{(i,\ j)}(1 - P_x^k(i,\ j)^2 - P_y^k(i,\ j)^2) \\
&\quad + \frac{\lambda}{2}P_x^k(i,\ j)\left(\frac{\partial v_x}{\partial y} + \frac{\partial v_y}{\partial x}\right)^k(i,\ j)(1 - P_x^k(i,\ j)^2 - P_y^k(i,\ j)^2)
\end{aligned}
$$

and

$$
\begin{aligned}
& f(P_y^{k+1/2}(i,\ j)) \\
&= -V_y(i,\ j)\frac{P^{k+1/2}_{y(i,\ j+1)} - P^{k+1/2}_{y(i,\ j-1)}}{2\Delta y} + \frac{1}{2}P_x^k(i,\ j)\left(\frac{\partial v_y}{\partial x} - \frac{\partial v_x}{\partial y}\right)^k(i,\ j) \\
&\quad + \lambda P_y^{k+1/2}(i,\ j)\frac{\partial v_y}{\partial y}\Bigg)^k_{(i,\ j)}(1 - P_x^{k+1/2}(i,\ j)^2 - P_y^k(i,\ j)^2) \\
&\quad + \frac{\lambda}{2}P_x^k(i,\ j)\left(\frac{\partial v_x}{\partial y} + \frac{\partial v_y}{\partial x}\right)^k(i,\ j)(1 - P_x^{k+1/2}(i,\ j)^2 - P_y^k(i,\ j)^2).
\end{aligned}
$$

3.2.4. Orientation tensors

Equation (14) becomes

$$\frac{\partial a_{11}}{\partial t} = f(a_{11})$$

with

$$f(a_{11}) = -v_x\frac{\partial a_{11}}{\partial x} - v_y\frac{\partial a_{11}}{\partial y} - 2\lambda\Omega_{kl}A_{11kl}.$$

According to the second-order Runge-Kutta method, this equation is written as:

$$a_{11}^{k+1}(i,\ j) = a_{11}^{k}(i,\ j) + \Delta t f(a_{11}^{k+1/2}(i,\ j))$$

or

$$a_{11}^{k+1/2}(i,\ j) = a_{11}^{k}(i,\ j) + \frac{\Delta t}{2} f(a_{11}(i,\ j))$$

with

$$f(a_{11}^{k}(i,\ j)) = -V_x(i,\ j)\frac{a_{11(i+1,\ j)}^{k} - a_{11(i-1,\ j)}^{k}}{2\Delta x} - V_y^{k}(i,\ j)\frac{a_{11(i,\ j+1)}^{k} - a_{11(i,\ j-1)}^{k}}{2\Delta y} - 2\lambda\Omega_{kl}A_{11kl}\Bigg)_{(i,\ j)}^{k}$$

and

$$f(a_{11}^{k+1/2}(i,\ j)) = -V_x(i,\ j)\frac{a_{11(i+1,\ j)}^{k+1/2} - a_{11(i-1,\ j)}^{k+1/2}}{2\Delta x} - V_y^{k}(i,\ j)\frac{a_{11(i,\ j+1)}^{k+1/2} - a_{11(i,\ j-1)}^{k+1/2}}{2\Delta y} - 2\lambda\Omega_{kl}A_{11kl}\Bigg)_{(i,\ j)}^{k}.$$

Equation (15) becomes

$$\frac{\partial a_{12}}{\partial t} = f(a_{12})$$

with

$$f(a_{12}) = -v_x\frac{\partial a_{12}}{\partial x} - v_y\frac{\partial a_{12}}{\partial y} + \left[\frac{1}{2}\frac{\partial v_y}{\partial x}(1+\lambda) + \frac{1}{2}\frac{\partial v_x}{\partial y}(1-\lambda)\right]a_{11} + \left[\frac{1}{2}\frac{\partial v_y}{\partial x}(\lambda-1) - \frac{1}{2}\frac{\partial v_x}{\partial y}(\lambda+1)\right]a_{22} - 2\lambda\Omega_{kl}A_{12kl}.$$

According to the second-order Runge-Kutta method, this equation is written as:

$$a_{12}^{k+1}(i,\ j) = a_{12}^{k}(i,\ j) + \Delta t f\left(a_{11}^{k+1/2}(i,\ j)\right)$$

or

$$a_{12}^{k+1/2}(i,\ j) = a_{12}^{k}(i,\ j) + \frac{\Delta t}{2} f\left(a_{12}(i,\ j)\right)$$

with

$$\begin{aligned} & f\left(a_{12}^{k}(i,\ j)\right) \\ &= -V_x(i,\ j)\frac{a_{12(i+1,\ j)}^{k} - a_{12(i-1,\ j)}^{k}}{2\Delta x} - V_y^{k}(i,\ j)\frac{a_{12(i,\ j+1)}^{k} - a_{12(i,\ j-1)}^{k}}{2\Delta y} \\ &+ \left[\frac{1}{2}\frac{\partial v_y}{\partial x}(i,\ j)(1+\lambda) + \frac{1}{2}\frac{\partial v_x}{\partial y}(i,\ j)(1-\lambda)\right]_{(i,\ j)}^{k} a_{11}^{k}(i,\ j) \\ &+ \left[\frac{1}{2}\frac{\partial v_y}{\partial x}(\lambda-1) - \frac{1}{2}\frac{\partial v_x}{\partial y}(\lambda+1)\right]_{(i,\ j)}^{k} a_{22}^{k}(i,\ j) - 2\lambda\Omega_{kl}A_{12kl}\Bigg)_{(i,\ j)}^{k} \end{aligned}$$

and

$$\begin{aligned} & f\left(a_{12}^{k+1/2}(i,\ j)\right) \\ &= -V_x(i,\ j)\frac{a_{12(i+1,\ j)}^{k+1/2} - a_{12(i-1,\ j)}^{k+1/2}}{2\Delta x} - V_y^{k}(i,\ j)\frac{a_{12(i,\ j+1)}^{k+1/2} - a_{12(i,\ j-1)}^{k+1/2}}{2\Delta y} \\ &+ \left[\frac{1}{2}\frac{\partial v_y}{\partial x}(i,\ j)\left(1 + (1+\lambda) + \frac{1}{2}\frac{\partial v_x}{\partial y}\right)(i,\ j)\right]_{(i,\ j)}^{k} a_{11}^{k}(i,\ j) \\ &+ \left[\frac{1}{2}\frac{\partial v_y}{\partial x}(\lambda-1) - \frac{1}{2}\frac{\partial v_x}{\partial y}(\lambda+1)\right]_{(i,\ j)}^{k} a_{22}^{k}(i,\ j) - 2\lambda\Omega_{kl}A_{12kl}\Bigg)_{(i,\ j)}^{k}. \end{aligned}$$

Equation (16) becomes

$$\frac{\partial a_{22}}{\partial t} = f(a_{22})$$

with

$$f(a_{22}) = -V_x \frac{\partial a_{22}}{\partial x} - V_y \frac{\partial a_{22}}{\partial y} - 2\lambda\Omega_{kl} A_{22kl}.$$

According to the second-order Runge-Kutta method, this equation is written as:

$$a_{22}^{k+1}(i,\ j) = a_{22}^{k}(i,\ j) + \Delta t f(a_{22}^{k+1/2}(i,\ j))$$

or

$$a_{22}^{k+1/2}(i,\ j) = a_{22}^{k}(i,\ j) + \frac{\Delta t}{2} f(a_{22}(i,\ j))$$

with

$$f(a_{22}^{k}(i,\ j)) = -V_x(i,\ j)\frac{a^k_{22(i+1,\ j)} - a^k_{22(i-1,\ j)}}{2\Delta x} - V_y^k(i,\ j)\frac{a^k_{22(i,\ j+1)} - a^k_{22(i,\ j-1)}}{2\Delta y} - 2\lambda\Omega_{kl} A_{22kl}\Bigg)^{k}_{(i,\ j)}$$

and

$$f(a_{22}^{k+1/2}(i,\ j)) = -V_x(i,\ j)\frac{a^{k+1/2}_{22(i+1,\ j)} - a^{k+1/2}_{22(i-1,\ j)}}{2\Delta x} - V_y^k(i,\ j)\frac{a^{k+1/2}_{22(i,\ j+1)} - a^{k+1/2}_{22(i,\ j-1)}}{2\Delta y} - 2\lambda\Omega_{kl} A_{22kl}\Bigg)^{k}_{(i,\ j)}.$$

All the terms of the non-principal partial variables are discretized or centered by the finite difference method.

Calculations are started using an initial profile that fulfills the limit conditions. Use of these values enables the determination of temperature profiles, fluid velocity, definition of orientation and tensor orientation of short fibers. Both algebraic equations are solved by means of a numerical code in FORTRAN and the results and their interpretations are given in the following part.

3.2.5. Image processing methodology

Analysis by Matlab

We analyze three samples of polypropylene.

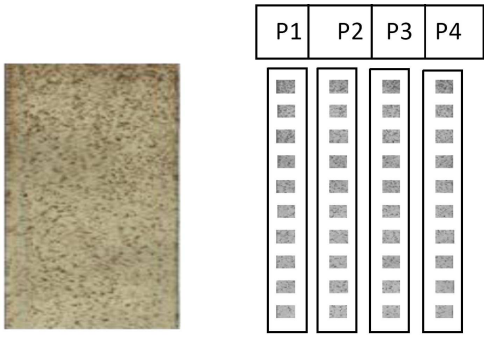

Figure 3. Rectangular sample containing polypropylene mixed with short fibers.

Image processing and image analysis were carried out using an internal software built with Matlab and an image processing toolkit (IPT). A detection system was designed to measure the very elliptical footprint, based on manual or semi-manual selection.

The implemented algorithm included the following general steps: collection, discretization and imprint characterization, correction flat angles, and average fiber orientation calculation.

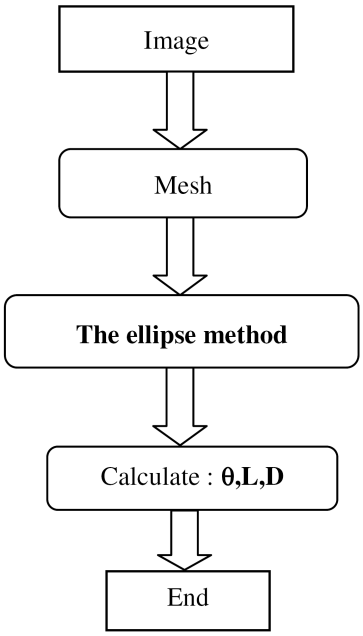

Figure 4. Organigram.

3.2.6. Results

In Figures 5 and 6, we show the evolution of the tensor orientation as a function of the x axis and time, with the measurements, the results are again well accepted. Compared to the previous isothermic case, the direction upstream of the flow front is not changed with a non-isothermal Newtonian behaviour. The temperature effect in the fiber flow becomes important during the travel, and in isothermal conditions, the final z position is lower. Particles migrate towards the wall with the non-isothermal shear thinning behaviour, as soon as they reach the cavity. The displacement in the flow front region in the direction of the gap towards the wall requires a longer distance than in the Newtonian case but the final position in the thickness is the same. Figure 3 shows the path evolution of a fiber entering the cavity, with an interaction coefficient $ci = 20$ under Newtonian isothermal

conditions. The first a_{22} increases, and a_{12} and a_{11} decrease: the fibers orient in the direction of flow z because of the shear flow. At the beginning of the fountain surge, the a_{22} reduces and the fibers are mainly directed towards the x direction. As the fibers hit the wall, they reorient themselves towards motion.

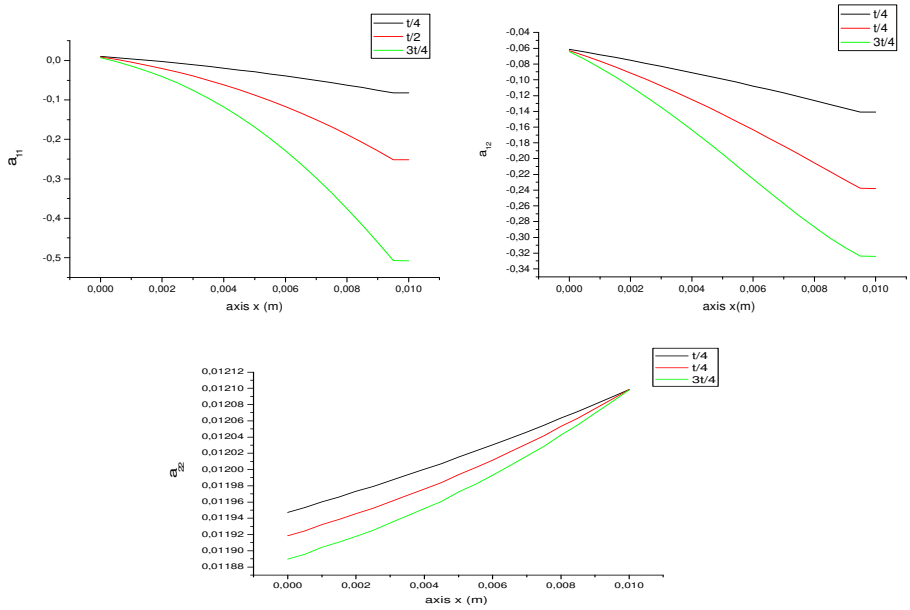

Figure 5. The variation of the orientation tensor as a function of the x axis.

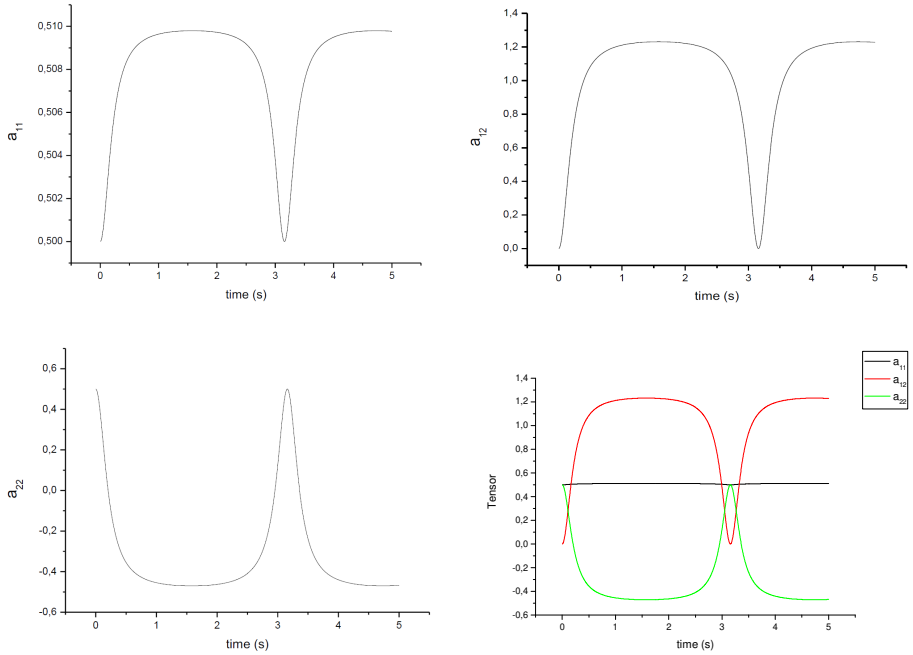

Figure 6. The variation of the orientation tensor as a function of time.

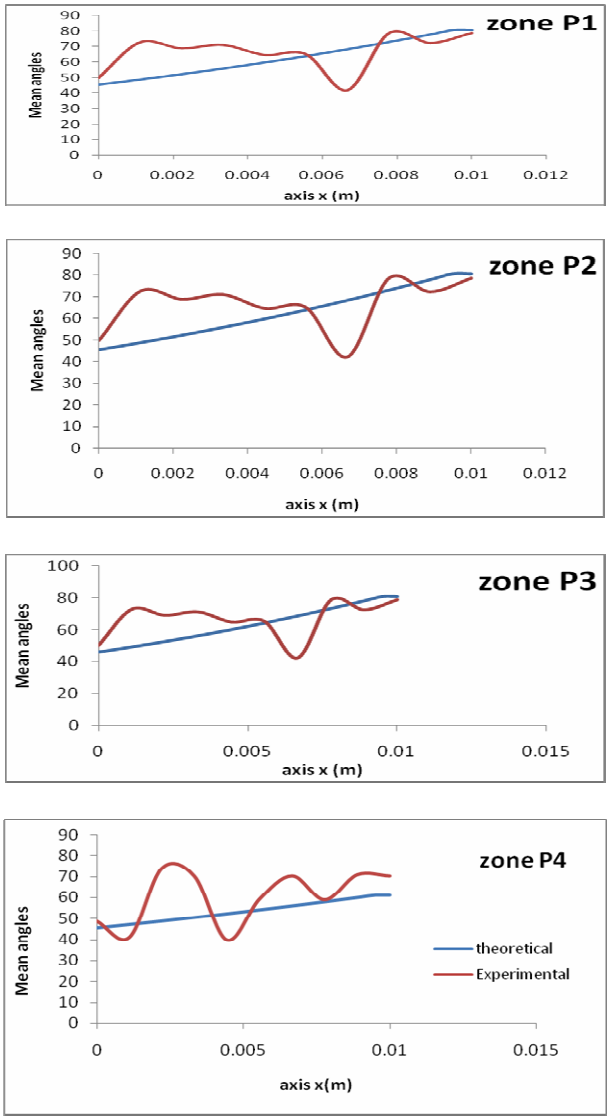

Figure 7. Profile of the orientation angle as a function of the *x* axis.

Figure 7 provides a description of the axis *x* orientation progression between the experimental and theoretical results for the four positions P1, P2, P3 and P4. Review of results from numerical simulation and experience indicates a small difference between the two curves.

This difference can be explained by the fact that in experimental experiments, a lot of factor can play a role in affecting such as fiber-fiber communication, as well as by a narrower mesh as opposed to theoretical one.

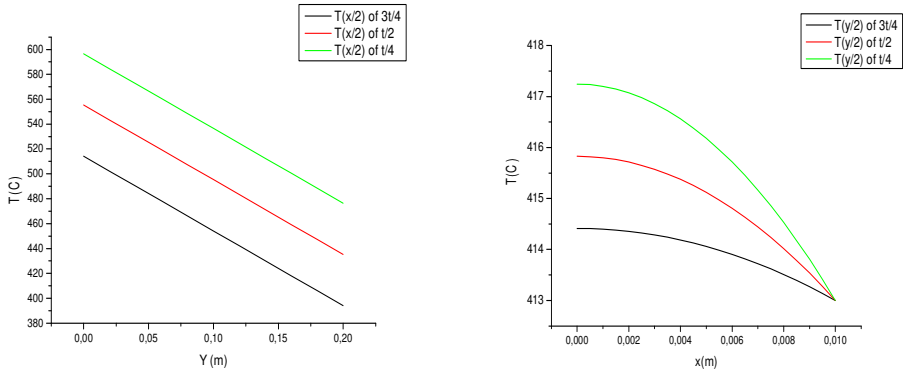

Figure 8. Profile of the temperature as a function of the x, y and time axes.

In this figure, we see that the temperature in time decreases at times $(t = T/4,\ \ t = T/2$ and $t = 3T/4)$ as a function of sample width (l) and length (L). It is noted that as the polymer passes forward through the container, the temperature amplitudes decrease. It can be explained by assuming that the polymer is more liquid and thus the ions are untangled and can roll over one another easily inducing temperature changes.

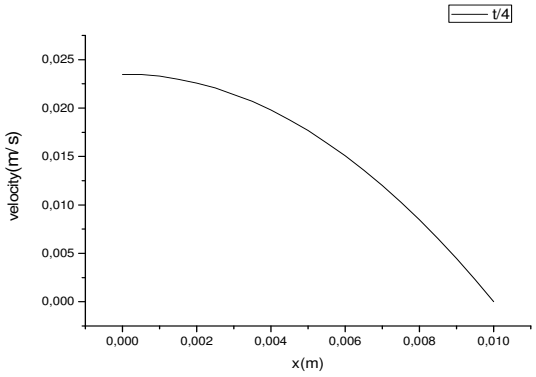

Figure 9. Profile of the axial speed as a function of the variable x.

This chart displays the variation in the axial velocity as a result of measured plate width *x*. The axial velocity is seen to diminish as time passes. This finding can be explained by the fact that the particles are slightly pushed from their equilibrium position near the wall and complicated molecular motions, which results in a decrease in the volume of axial velocity.

4. Conclusion

In this paper, we present the difference in the fiber orientation distribution during flow molding of a composite polypropylene reinforced by short fiber. Jeffery's equation has been adopted to explain the rotational motion of a single fiber, in which the interaction between the fibers is ignored. The distribution of the fiber orientation along the flow distance is determined by assuming a two-random dimensional distribution at start-up of flow. If the flow is a fully formed shear flow in a steady state between parallel sheets, then the prediction of variance of the fiber orientation distribution is implemented in the shear flow. The analytical results showed that as the flow distance increases, the fibers tend to be arranged in such a way that they become steadily parallel to the flow path. The prediction of variance of the distribution of orientation of the fibers in the radial flow is also carried out. The study has shown that the fibers tend to be formed in such a way as to become progressively more perpendicular to wind direction. The pattern is verified compared to an experimental sample.

Acknowledgement

The authors are highly grateful to the referee for his careful reading, valuable suggestions and comments, which helped to improve the presentation of this paper.

References

[1] G. B. Jeffery, The motion of ellipsoidal particles immersed in a viscous fluid, Proceedings of the Royal Society of London, Series A 102(715) (1922), 161-179.

[2] G. G. Lipscomb, Analysis of suspension rheology in complex flows, Ph.D. dissertation, University of California, Berkeley, 1987.

[3] M. Vincent, E. Devilers and J. F. Agassant, Fiber orientation in injection molding of reinforced thermoplastics, Journal of Non Newtonian Fluid Mechanics 73 (1997), 317-326.

[4] F. Folgar and C. L. Tucker, Orientation behavior of fibers in concentrated suspensions, J. Reinf. Plast. Compos. 3 (1984), 98-119.

[5] S. Prager, Stress-strain relation in a suspension of dumbbells, Trans. Soc. Rheol. 1 (1994), 53.

[6] G. L. Hand, A theory of anisotropic fluids, J. Fluid Mech. 13 (1962), 33-46.

[7] R. S. Bay, Fiber orientation in injection-molded composites: a comparison of theory and experiment, Ph. D. dissertation, University of Illinois at Urbana-Champagne, 1991.

[8] C. Carrot and J. Guillet, Viscoélasticité non linéaire des polymères fondus, Traité Plastiques et Composites, 1999.

[9] A. Chapman, Y. Saad and L. Wigton, High order ILU preconditioners for CFD problems, Rapport technique, AMSI, Minnesota Supercomputer Institute, 1996.

[10] A. J. Chorin, Numerical solution of the Navier-Stokes equations, Math. Comp. 22 (1968), 745-762.

[11] S. G. Advani and C. L. Tucker, A numerical simulation of short fiber orientation in compression molding, Polym. Compos. 11 (1990), 164-173.

[12] M. C. Altan, S. Subbiah, S. I. Guceri and R. B. Pipes, Numerical prediction of three dimensional fiber orientation in Hele-Shaw flows, Po1ym. Eng. Sci. 30 (1990), 848-859.

[13] I. Modhaffar, K. Gueraoui, H. El-Tourroug and S. Men-La-Yakhaf, Numerical study of short fiber orientation in simple injection molding processes, AIP Conf. Proc. 1653 (2015), 020071.

[14] I. Modhaffar, K. Gueraoui, S. Men-La-Yakhaf, H. El-Tourroug, M. Taibi, M. Driouich, M. Sammouda and M. Belcadi, Simulation and prediction of the orientation of short fibers polypropylene injected into a matrix with the imaging technique (HFSP), to appear.

[15] J. C. Halpin and J. L. Kardos, Strength of discontinuous reinforced composites: 1 fiber reinforced composites, Polym. Eng. Sci. 18 (1978), 496-500.

[16] S. H. McGee, The influence of microstructure on the elastic properties of composite materials, Ph. D. Thesis, University of Delaware, Newark, 1982.

[17] I. Modhaffar, K. Gueraoui, S. Men-La-Yakhaf and H. El-Tourroug, The effect of orientation of short fibers in the diluted suspension for thermoplastic, International Review of Mechanical Engineering (IREME) 10(1) (2016), 7-11.

[18] A. Clarke, N. Davidson and G. Archenhold, Measurements of fibre direction in reinforced polymer composites, Journal of Microscopy 171(1) (1993), 69-79.

[19] C. Eberhardt and A. R. Clarke, Fibre orientation measurements in short glass fiber composites: I automated high angular resolution measurement by confocal microscopy, Composite Sciences Technology 61 (2001), 1389-1400.

[20] S. Men-La-Yakhaf, K. Gueraoui and M. Driouich, New numerical and mathematical code reactive mass transfer and heat storage facilities of argan waste, Advanced Studies in Theoretical Physics 8(10) (2014), 485-498.

[21] H. El-Tourroug, K. Gueraoui, N. Hassanain, I. Modhaffar and S. Men-La-Yakhaf, Numerical and mathematical modeling of the injection for incompressible fluids through rigid cylindrical duct: application of melted polymers PPH, Appl. Math. Sci. 8(180) (2014), 8953-8964.

[22] I. Modhaffar, K. Gueraoui, S. Men-La-Yakhaf and H. El-Tourroug, Simulation study for prediction of short fiber orientation reinforced thermoplastics, Materials Today: Proceedings 3 (2016), 2891-2897.

[23] S. Men-La-Yakhaf, K. Gueraoui, A. Maaouni and M. Driouich, Numerical and mathematical modeling of reactive mass transfer and heat storage installations of argan waste, International Review of Mechanical Engineering (IREME) 8(1) (2014), 236-240.